



that in solution,  $\Delta T$ , increases with time, being initially at *ca* 2<sup>o</sup>C and reaching a value as high as *ca* 17<sup>o</sup>C two hours later. The increase in the surface temperature, curve a, is irregular indicating bursts in excess enthalpy generation. In contrast, the solution temperature, curve b, increases smoothly which is an expected behavior because the weight (volume) of solution exceeds that of the Pd/D electrode assembly.

### 2.2 Development of hot spots

Thermal activity in the form of “hot spots”, Figs. 4a – 4d, were detected early during the Pd/D co-deposition process. We note that (i) the rate of heat generation is not uniform, (ii) thermal activities occur at low cell temperature and at low cell currents, (iii) the intensity of thermal activity increases with an increase in both cell temperature and cell current, Fig. 5. Here, the temperature of hot spots cannot be estimated because it exceeded the camera range.

## 3.0 Lattice distortion

An expected consequence of localized heat sources is lattice distortion and the development and propagation of stresses within the Pd/D lattice. The display of mechanical distortion can be followed by co-depositing the Pd/D films onto pressure sensitive substrates, *eg* piezoelectric ceramic material[2]. To eliminate external factors that might interfere with the interpretation of the sensor’s response the electrochemical cell was shielded (Faraday cage) and the whole assembly placed on a shock absorbing material, as illustrated in Fig. 6.

### 3.1 Single events

An ideal response of a piezoelectric sensing device to thermal mini-explosion is illustrated in Fig. 7. A single isolated event is shown in Fig. 8a. Here, we see clearly a single voltage spike which, in the negative direction, corresponds to the pressure pulse. After a brief period of time,  $\Delta t = 0.06$  sec., we note the arrival of the temperature front (voltage spike in the opposite direction), followed by the system relaxation. Using a simple model, *eg* that of a spherical reaction site, one could, from the magnitude of the voltage spikes and the  $\Delta t$ , reach some conclusion concerning the position and strength of the heat source. Such singular events are seen in the early periods of the co-deposition. Interestingly, these voltage bursts persisted for hours following the termination of current flow.

### 3.2 Bursts

A typical voltage-time behavior indicating a burst of events within the Pd/D film is shown in Fig. 8b. These bursts were observed at constant current densities as low as *ca* 4.0  $\mu\text{Acm}^{-2}$ . An expanded trace of such bursts shows a series of voltage spikes, indicated by arrows. Their frequency and intensity increased with an increase in the cell current and cell temperature. At temper-

ature near the boiling point, thermal activities were very intense as indicated by the magnitude of the voltage spikes, illustrated in Fig. 9.

#### 4.0 Discussion

The appearance of discrete reaction sites implies the transition from a stable to an unstable regime, alternatively a transition from non-reactive to reactive sites. We regard the formation of these domains as being the last step prior to the initiation of the F-P effect. Furthermore, we define a reference state in which all flow of matter is stopped but the flow of energy is permitted. The reference state is maintained by an overpotential, alternatively, by the cell current. In the reference state in which all octahedral sites are occupied, the overpotential acts as an external potential, *ie* it determines the distribution of all mobile charges (both  $D^+$  and  $e^-$ ). The vanishing of all mass fluxes demands that all chemical potentials within the Pd/D system be equal.

We examine the associated dynamics leading to the instabilities of what should otherwise be stable behavior, *via* (i) the construction of an interphase across which deuterium transport occurs, and (ii) the system's response to perturbations in the cell current/potential.

##### 4.1 Construction of the Pd/D<sub>2</sub>O interphase

Here, as in an earlier communication[1], we follow closely the procedure outlined by van Rysselberghe[3]. Briefly, the interphase region consists of a set of non-autonomous layers where the overall overpotential can be broken into parts pertaining to the various layers and where these layers are determined by the sequence of processes/reactions. Each layer of the set of non-autonomous layers is homogeneous and of sufficiently large volume so that the concentration and temperature are well defined and their location is given by the driving forces, the chemical potentials. The structure of the Pd/D-D<sub>2</sub>O interphase arises from the set of steps involved in the electrochemical charging *viz* electroreduction of  $D^+$  ions in the reaction layer, followed by adsorption, absorption, placement in the Pd lattice, ionization (dissociation), and transport into the bulk metal, Fig.10.

Restricting our attention to the relevant part of the structure of the interphase and the processes therein, we examine the dynamics of the Pd/D-D<sub>2</sub>O system under the following set of assumptions: (i) the  $e^-$ 's are treated as a component as are the  $D^{(\theta)}$ ,  $D^{(a)}$ ,  $D^{(\lambda)}$ ,  $D^+$  species[4], (ii) the transition from  $D_{ad}$  to  $D_{ab}$  is fast so that during charging they remain in quasi-equilibrium, (iii) ionization,  $D_l \rightleftharpoons D^+ + e^-$ , is considered a chemical reaction occurring in a  $s^-$  electron rich environment.

##### 4.2 Stability with respect to overpotential variation

The negatively polarized Pd/D electrode of an operating electrochemical cell is a

complex system. Its behavior with respect to perturbation in the overpotential,  $\eta$ , will be first examined by considering a set of thought experiments in which a closed system containing D, D<sup>+</sup> and e<sup>-</sup> at equilibrium will be subjected to (i) action of an external potential,  $\eta$ , (ii) the addition of electrons in the absence of  $\eta$ , and (iii) addition of electrons in the presence of  $\eta$ .

(i) The external potential affects only charged species *via* the internal potential,  $\chi$ . If the system contains an equal number of positively and negatively charged particles, then the action of an external potential is canceled.

(ii) If the number of negatively charged particles is greater than the number of positively charged (e.g. by addition of electrons) then the addition of negatively charged particles increases the chemical potential,  $\mu^{(r)}$ , due to an increase in the second term of Eq. (2). The net result is the decrease in the concentration of positively charged particles.

(iii) The action of the external potential on the system with unequal number of charged particles is more complex. In the system where the negative charges exceed the positive, the net result is the decrease of the  $\mu^{(r)}$  (Note – logarithmic term in Eq. (2) changes slower than the linear term). The composition of the *quasi-equilibrium* is determined by both the excess of negative particles and the magnitude of the applied potential, i.e.  $\mu^{(r)} = f[q_-, \chi]$ . As the external potential is increased, the  $\mu_+^{(r)}$  also increases.

In assessing the response to the variation in overpotential we take note of condition (iii). In addition, we assume that the surface coverage remains constant, *ie* that the extra cell current is used exclusively for the deuterium evolution reaction. Thus, condition (iii) yields

$$\mu^{(r)} = \bar{\mu}_+^{(r)} + \bar{\mu}_-^{(r)} \quad (1)$$

with

$$\bar{\mu}_{(+,-)} = \bar{\mu}_{(+,-)}^0 + RT \ln c_{(+,-)} + zq_{(+,-)}|\chi| \quad (2)$$

where  $c_{(+,-)}$  are the volume concentrations,  $q_{(+,-)}$ , is the charge density and  $\chi$  is the internal potential. The subscripts +,- refer to deuterons and s-electrons, respectively and the superscripts identify the layer under consideration.

Even a small deviation from the reference state results in instability. By definition,  $\mu = \partial U / \partial n|_{S,V,n,\dots}$ . Consequently, the stability/instability of the Pd/D system with respect to varying overpotential is determined by taking the derivative of the chemical potential. The chemical potential of the adsorption layer depends linearly on overpotential[5], *ie*  $\mu^{(\theta)}(\eta) = \mu^{(\theta)} + |\eta|F$  and  $\mu^{(r)} = \bar{\mu}_+^{(r)} + \bar{\mu}_-^{(r)}$ . Substitution of (2) into (1), followed by differentiation, yields

$$\frac{\partial \mu^{(r)}}{\partial \chi} = q_+ - q_- \quad (3)$$

Since  $\partial\mu^{(r)}/\partial\chi < 0$ , so is also  $\delta U < 0$ , *ie* the system is unstable with respect to the variation in overpotential.

### 4.3 Formation of active domains

The review of the thermal behavior suggests the following:

(i) The discrete heat sources were noted shortly after the initiation of current flow. Thus, they are located near the contact surface and the supercharged layer, in which  $[D]/[Pd] > 1$ , is formed instantaneously[6].

(ii) The nuclear active site must contain a large number of single events to produce a visible image. Unfortunately, our experimental set-up could not yield quantitative assessment. However, based on other considerations the estimated the number of single events to be between *ca*  $10^4 - 10^9$ .

(iii) The random time/space distribution of hot spots as well as their varying intensity with time, Figs. 4a–4d, exclude the existence of fixed location of the nuclear-active-sites. The random distribution and the varying intensity arises from the coupling of the various processes occurring on both sides of the contact surface in response to fluctuations.

(iv) Both, the frequency and intensity are a strong function of temperature. In particular, both increase with an increase in temperature, exhibiting the so-called positive feedback, *cf* Figs. 3 and 5. This is, perhaps, the most direct indication of the influence of the chemical environment.

To reiterate, active domains containing several thousands of particles are formed in the close proximity to the contact surface. The random distribution suggests that the beginnings of the new phase are generated as a result of fluctuations, while the strong temperature dependency attests to the action of forces of a chemical nature. In earlier communications[1,7], we pointed out that changes in an external force, e.g. the overpotential, substantially affects the dynamic behavior as well as the structure of the interphase which contains complexes of the form  $[D\dots D]^+$ . In a system containing high  $D^+/Pd$  ratio in a s-electron rich atmosphere (according to Preparata[8], *ca* 40 % of the metal volume is occupied by the s-electrons) and assisted by a high external potential, the high value of the  $\mu_+^{(r)}$  promotes the formation of deuteron clusters, possibly of the form  $[D_n^+ \cdot e_m^-]$ . Evidently, the s-electrons play a dominant role in the formation of an assembly of complexes,  $[D_n^+ e_m^-]$ .

### 5.0 Concluding remarks

The last step in the series of consecutive events leading to the F-P effect is the formation of active domains, the seats of the reaction(s), yielding an excess enthalpy. The arguments presented here arise from the following statements:

(i) The electrode/electrolyte interphase is viewed as an assembly of a set of

homogeneous layers identified by the processes occurring therein or with the associate chemical/electrochemical potentials.

(ii) The ionization (dissociation) of D in the Pd lattice is a chemical reaction (mass action law is obeyed, the chemical potential is the sum of the electrochemical potentials of constituents, *etc*)

(iii) the s-electrons play a dominant role in both, the high values of  $\bar{\mu}_+$  as well as in the forming of  $[D_m^- \cdot e_n^-]$  complexes.

#### REFERENCES

- [1] Mosier-Boss P. A. and Szpak S., *Nouvo Cim.*, **112A** (1999) 577
- [2] Dea J., Mosier-Boss P. A. and Szpak S., *Thermal and pressure gradients in polarized Pd/D system*, American Physical Society Spring meeting, Indianapolis, IN, April 2002
- [3] van Rysselberghe P., *Some Aspects of the Thermodynamic Structure of Electrochemistry*, in *Modernn Aspects of Electrochemistry*, J O'M. Bockris ed., vol. 4, Plenum Press, New York 1966
- [4] Defay R., Prigogine I. and Bellamans A., *Surface Tension and Adsorption*, Longmans, Green & Co, Ltd. London, 1966
- [5] Conway, B. E. and Jerkiewicz, G. *Z. phys. Chem.*, **183** (1994) 281
- [6] Szpak S., Mosier-Boss P. A. and Gabriel C. J., *J. Electroanal. Chem.*, **365** (1994) 275
- [7] Szpak S., Mosier-Boss P. A., Scharber S. R. and Smith J. J., *J. Electroanal. Chem.*, **337** (1992) 147
- [8] Preparata G., *Trans. Fusion Technology*, **26** (1994) 397

## Figures

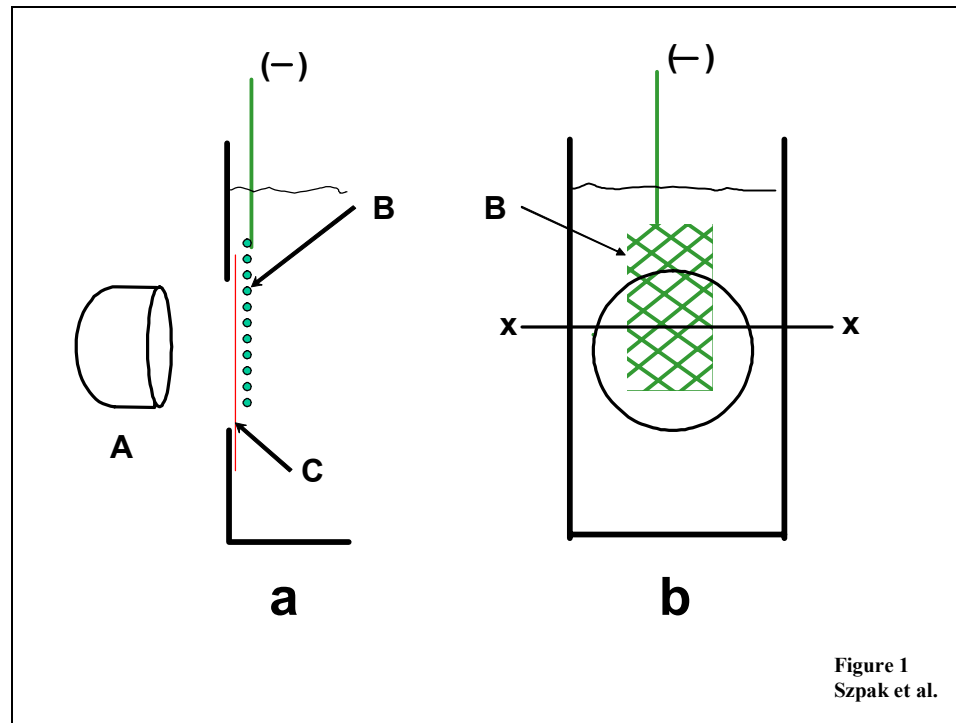


Figure 1. Experimental arrangement for infrared imaging. a (side view) - position of the IR camera; b (front view) - placement of the negative electrode (Ni screen): A - infrared camera, B - Ni screen, C Mylar film.

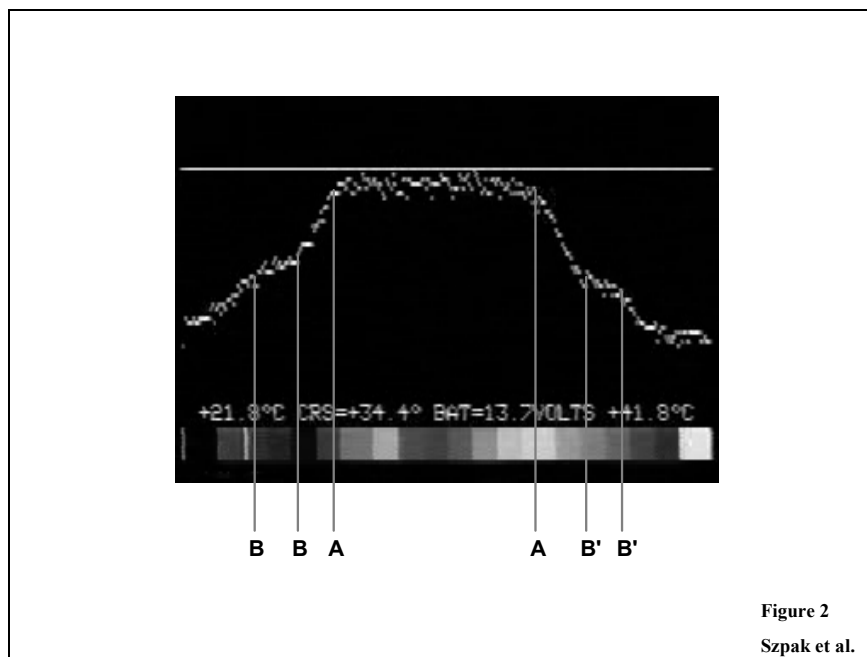


Figure 2  
Szpak et al.

Figure 2. Cell temperature profiles. A - A electrode surface temperature; B - B solution temperature.

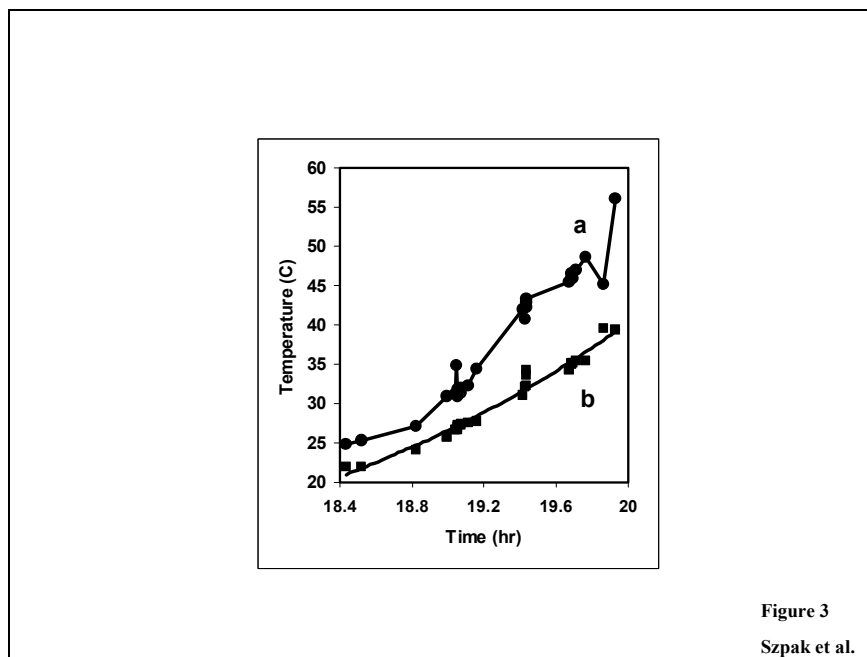


Figure 3  
Szpak et al.

Figure 3. Evolution of the temperature difference,  $\Delta T$ , as a function of time. a - electrode surface temperature; b - solution temperature.

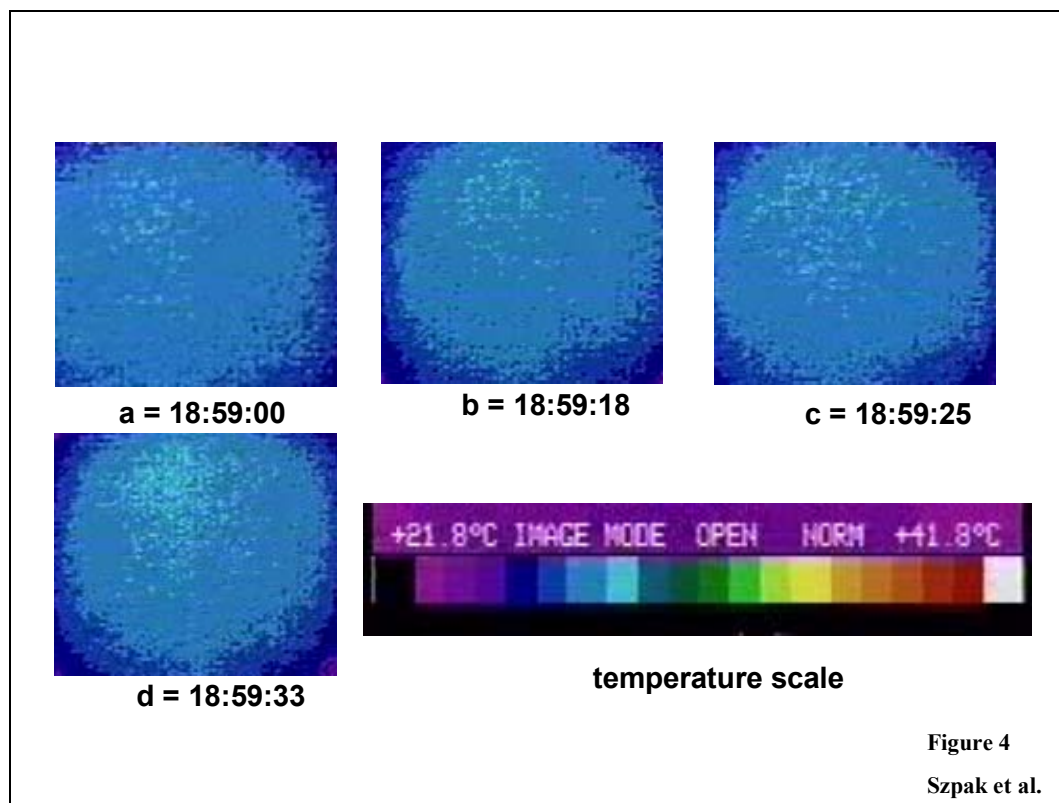


Figure 4. Time/space dependency of "hot spots", their intensity and frequency during co-deposition. Temperature scale included. "Hot spots" images at times indicated.

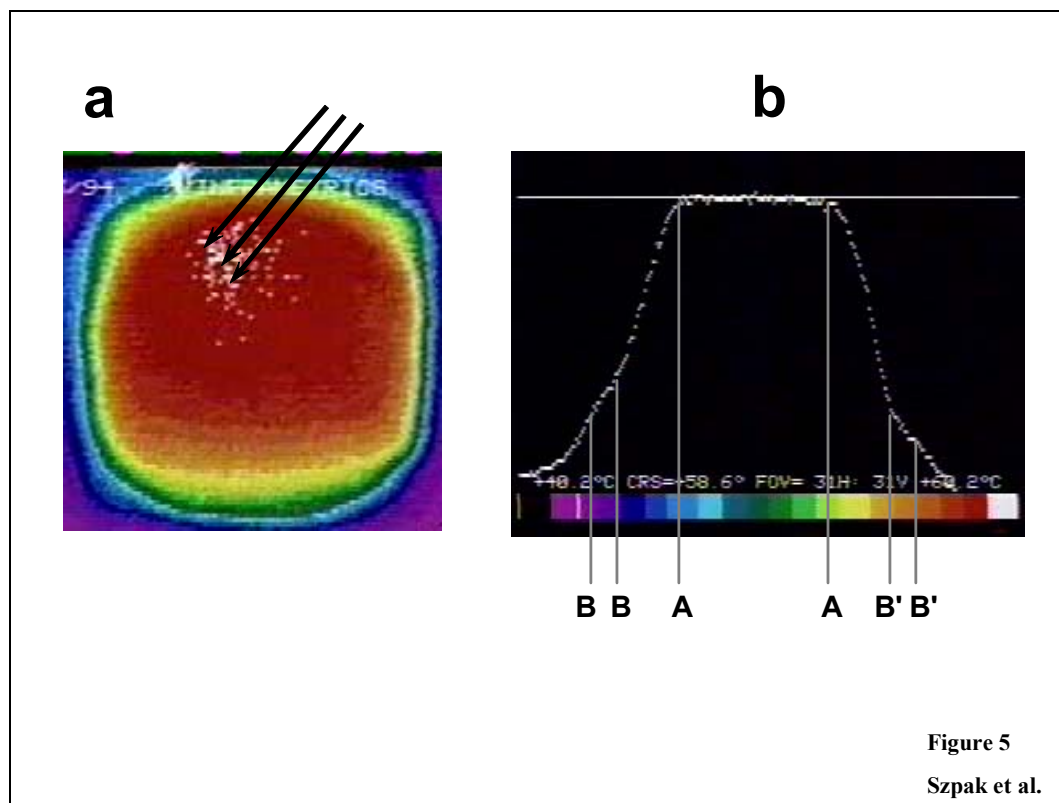


Figure 5  
Szpak et al.

Figure 5. Time/space dependency of “hot spots”. a - at elevated temperature; arrows indicated spots whose temperature was outside of the camera range; b - distribution of cell temperature. A-A electrode surface temperature, B-B solution temperature.

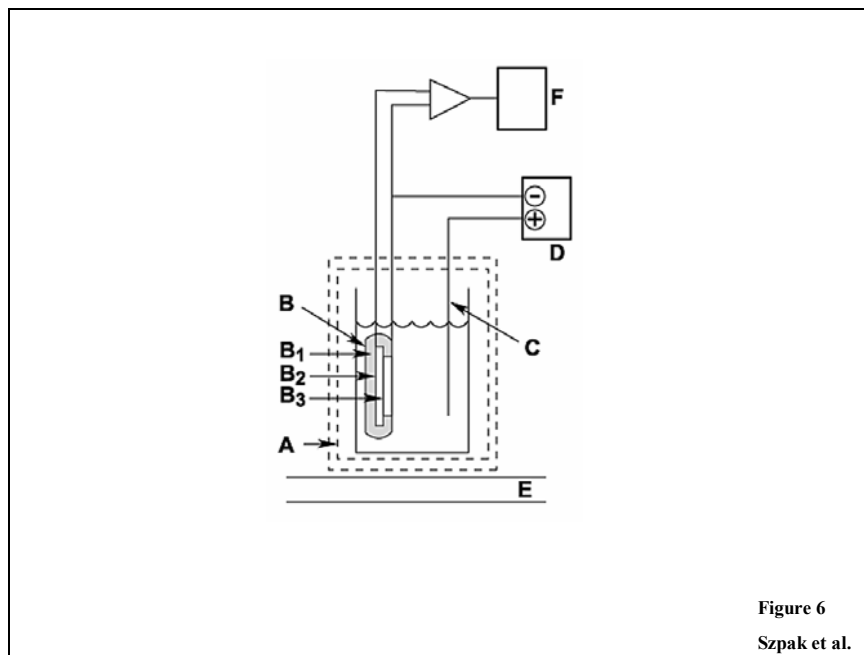


Figure 6  
Szpak et al.

Figure 6. Experimental arrangement for recording mini-explosions. A - Faraday cage, B - negative electrode assembly (B - insulating material, B - piezoelectric substrate, B - Pd/D film), C - positive electrode, D - potentiostat/galvanostat, E - shock absorbing material, F - oscilloscope (LeCroy digital), E - laboratory bench.

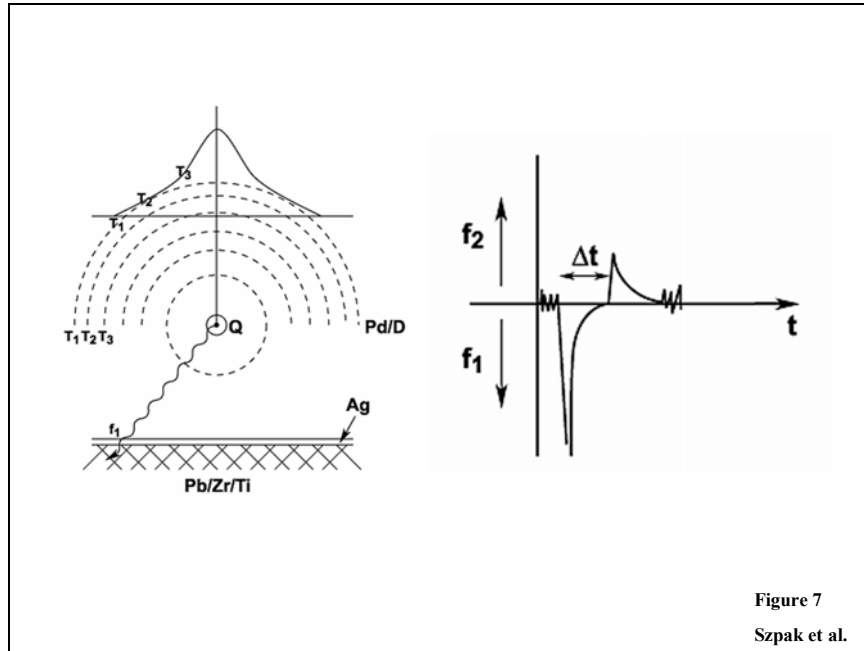
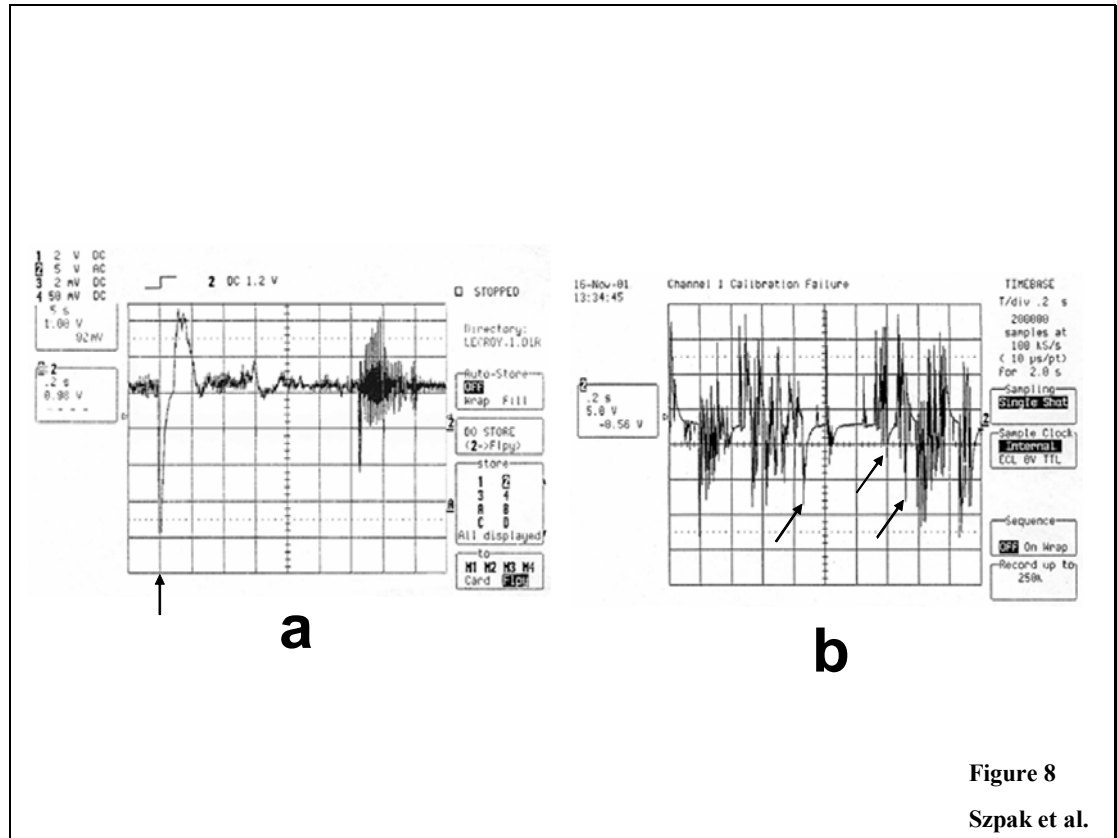


Figure 7  
Szpak et al.

Figure 7. Ideal representation of a mini-explosion. left - location of the instantaneous heat source and associated effects; right - a response of a piezoelectric sensor (f - compression, f - expansion).



**Figure 8**  
**Szpak et al.**

Figure 8. Typical response of a piezoelectric sensor. Left - A an isolated event. Right - B an expanded set of events, arrows indicate recognizable pattern.

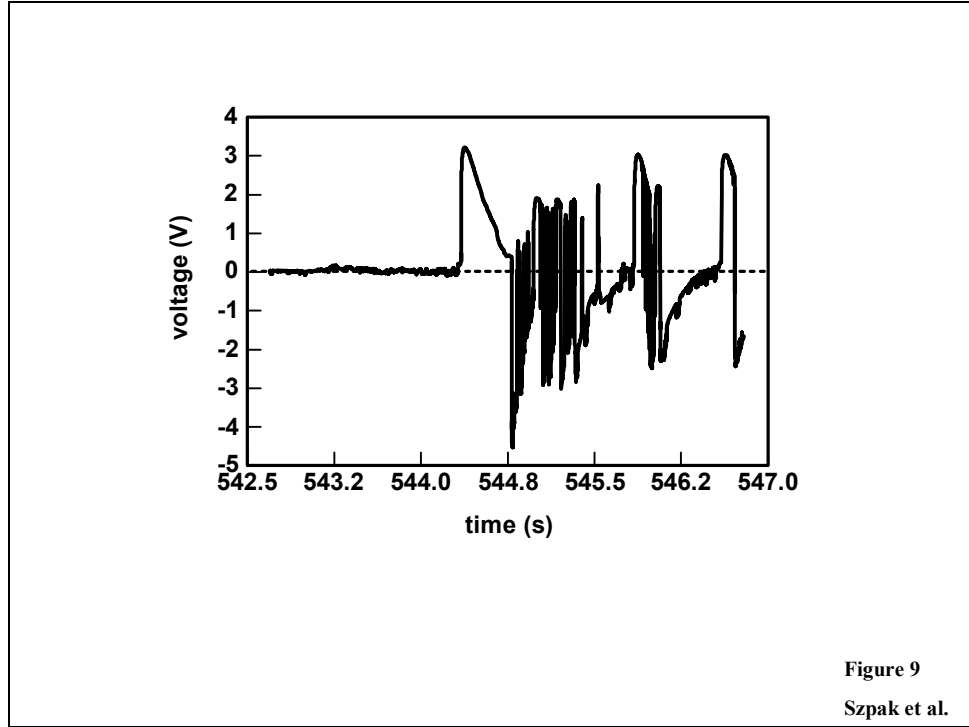


Figure 9. Response of a piezoelectric sensor to events occurring at the boiling point. The high voltage spikes (no amplification) indicate very strong pressure and temperature gradients activating the sensor's response.

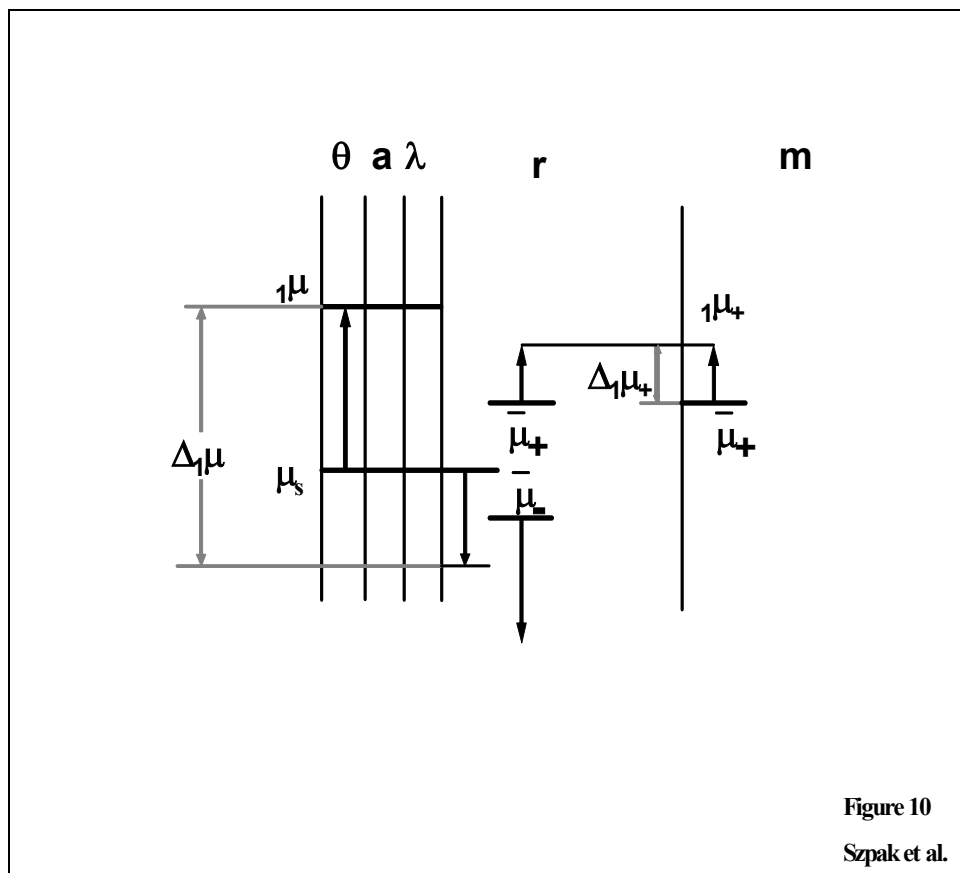


Figure 10  
Szpak et al.

Figure 10. Structure of the interphase. Layers:  $\theta$ – adsorption,  $a$  – adsorption,  $\lambda$ – lattice placement,  $r$  – reaction (dissociation),  $m$  – bulk metal;  $\mu_s$ – chemical/electrochemical potentials at the reference state (Equality  $\mu_s = \mu^{(\theta)} = \mu^{(a)} = \mu^{(\lambda)} = \mu^{(r)}$  and  $\bar{\mu}_+^{(r)} = \bar{\mu}_+^{(m)}$  refer to the stationary state). Chemical potentials  $1\mu^{(\theta)} = \dots$  are potentials associated with the change in the electrode overpotential. The equality  $1\mu^{(\theta)} = 1\mu^{(a)} = 1\mu^{(\lambda)}$  indicates fast adsorption  $\rightarrow$  absorption  $\rightarrow$  lattice placement.  $\Delta_1\mu$  and  $\Delta_1\bar{\mu}_+$  are the driving forces arising from the change in the electrode overpotential.